Active fault-tolerant control system against partial actuator failures

Y.M.Zhang and J.Jiang

Abstract: A novel approach for integrated fault detection, diagnosis and reconfigurable control systems design against actuator faults is proposed. The scheme is based on a two-stage adaptive Kalman filter for simultaneous state and fault parameter estimation, statistical decisions for fault detection, and activation of controller reconfiguration. Using the information from the fault detection and diagnosis scheme, the reconfigurable feedback controller is designed automatically based on an eigenstructure assignment technique. To eliminate the steady-state tracking error, a reconfigurable feedforward controller is also incorporated using a command generator tracker technique. The following fault types and input signals are considered: abrupt and incipient, single, multiple and consecutive faults, constant and arbitrarily varying reference inputs. The effectiveness and the superiority of the proposed approach are demonstrated using an aircraft example.

1 Introduction

Over the last two decades, the growing demand for reliability, maintainability, and survivability in aerospace systems and industrial processes has drawn significant research in fault detection and diagnosis (FDD) [1–6]. Such an effort has led to the development of many FDD techniques, although unfortunately, little attention was paid to fault-tolerant control (FTC) until the mid 1980s [7, 8]. More recently, the fault-tolerant control problem has started to attract more attention [9–14].

A fault-tolerant control system (FTCS) is a control system that possesses the ability to accommodate for system failures automatically and to maintain overall system stability and acceptable performance in the event of component failures. Generally speaking, fault-tolerant control systems can be classified into two types: passive and active. However, only an active FTCS against different degree of actuator failures is considered in this paper. In an active fault-tolerant control system, faults are detected and identified by a FDD scheme, and the controllers are reconfigured accordingly on-line in real-time. Through FDD, unforeseeable faults can be dealt with. Typically, a FTCS consists of three parts: a reconfigurable controller, a FDD scheme, and a control law reconfiguration mechanism. Key challenges are to design: (*a*) a sufficiently robust controller which is reconfigurable, (*b*) a FDD scheme with high sensitivity to faults and low sensitivity to disturbances, and (*c*) a reconfiguration mechanism which can recover the pre-fault system performance as much as possible. This paper will focus on the development of a new approach to such fault-tolerant control systems.

IEE Proceedings online no. 20020110

DOI: 10.1049/ip-cta:20020110

Paper first received 16th January and in revised form 15th October 2001

The authors are with the Department of Electrical and Computer Engineering, The University of Western Ontario, London, Ontario N6A 5B9, Canada

Existing reconfigurable controller design methods can be classified as: linear quadratic regulator (LQR) [8, 15, 16]; eigenstructure assignment (EA) [17]; adaptive control [18, 19]; pseudo-inverse [20]; model following [15, 21]; multiple-model [19, 22]; and neural networks and fuzzy logic [10, 14]. However, almost all of these methods assume that a perfect FDD result is already available, and a perfect post-fault model of the system is known. This is seldom the case in practice. Therefore, it is highly desirable to develop new techniques to integrate the FDD scheme and reconfigurable control law in a coherent fashion without any pre-assumption of the knowledge of the post-fault system. During the design process, the random measurement noises, uncertainties, impreciseness and time delay of FDD in the system should all be taken into consideration. Ideally, to perform the controller reconfiguration, the FDD scheme should provide detailed information on the post fault system as accurately as possible, and the controller should be able to achieve the optimal performance with the limited amount of information. The main objective of this paper is to show an interesting way to integrate FDD and FTCS to tolerant actuator failures.

The proposed approach uses a two-stage adaptive Kalman filter for simultaneous state and fault parameter estimation. The fault detection, diagnosis and activation of the controller reconfiguration are carried out based on statistical decisions. An on-line automatic reconfigurable controller design is based on both feedforward and feedback strategies. Fig. 1 depicts the general structure of this scheme.

In the fault detection and diagnosis module, both the actuator fault parameter and the system state variables are estimated via the two-stage adaptive Kalman filter [23]. On-line fault detection and diagnosis schemes are used to activate the control reconfiguration mechanism. Based on the up to date information of the post-fault system, an eigenstructure assignment technique is employed to design a reconfigurable feedback controller. To achieve steady-state tracking even in the presence of faults, a reconfigurable feedforward controller is also designed using the command generator tracker technique [24].

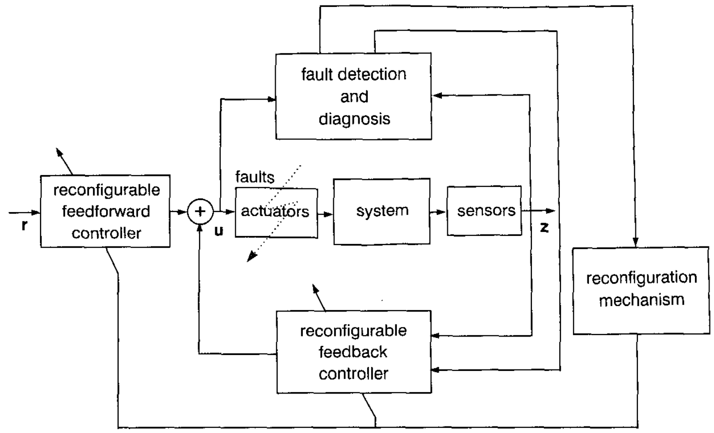

Fig. 1 *General structure of proposed fault-tolerant control system*

2 Modelling of actuator faults through control effectiveness

Actuators are the work-horses in a control system. They represent the links between the control commands issued by the controller and the physical actions performed to the system. For this reason, actuators are often known as final-control-elements, and they interact with the manipulated variables of the system directly. In practical systems, controllers and actuators are often located physically in different parts of the system. Depending on applications, actuators can be valves, solenoids, motors, etc. In the case of an aircraft, the actuators are often in the form of hydraulically-driven control surfaces. The objective of such control surfaces is to provide incremental lift force to control the aircraft. This can be achieved through deflecting appropriate flaps located in the different parts of the aircraft. For example, the flapped portion of the tail surface is known as an elevator, yaw control can be achieved by a flap on the vertical tail called the rudder, and the roll motion can be controlled by flaps towards the tips of the wings, known as ailerons. An example of such control surfaces is shown in Fig. 2.

During normal operation, the actuators would operate exactly as directed by the controller. We say that these actuators are 100% effective (in executing the control commands). When faults occur in actuators, such as partial loss of a control surface, or pressure reduction in hydraulic lines, in the case of an aircraft, partial blockage of a control valve in process control, or voltage reduction/amplifier saturations in electrical servo systems, the actuators would not be able to fulfill the control commands completely. In such cases, we say that the effectiveness of the actuators has been reduced.

This observation provides us with a possible way to quantify the severity of the actuator faults. This can be done through introduction of a parameter known as the reduction of the control effectiveness factor [23], which represents the loss of the one-to-one relationship between the control command (controller output) and the true actuator actions. Therefore, the actuator faults can be defined as any abnormal operation of any element in the actuator subsystem such that the control command from the controller output cannot be delivered to the manipulated variables entirely. An illustration is shown in Fig. 3.

We assume that the fault-free system can be described by the following model:

$$\begin{aligned} \mathbf{x}_{k+1} &= A\mathbf{x}_k + B\mathbf{u}_k + \mathbf{w}_k^{\mathbf{x}} \\ \mathbf{y}_k &= C_r\mathbf{x}_k \\ \mathbf{z}_k &= C\mathbf{x}_k + \mathbf{v}_k \end{aligned} \tag{1}$$

where $\mathbf{x}_k \in \Re^n$ is the system state, $\mathbf{u}_k \in \Re^l$ is the input, $\mathbf{y}_k \in \Re^p$ represents those system outputs that will track the reference inputs, $\mathbf{z}_k \in \Re^m$ corresponds to the measurements used in the Kalman filter, $\mathbf{w}_k^{\mathbf{x}}$ is a zero-mean white Gaussian noise sequence with covariance $Q_k^{\mathbf{x}}$ representing the modelling errors, $\mathbf{v}_k$ is a zero-mean white Gaussian measurement noise sequence with covariance R_k, and the initial state $\mathbf{x}_0$ is a Gaussian vector with mean $\bar{\mathbf{x}}_0$ and covariance $\bar{P}_0^{\mathbf{x}}$.

The system with actuator faults modelled by control effectiveness factors can then be written as:

$$\mathbf{x}_{k+1} = A\mathbf{x}_k + B_k^f\mathbf{u}_k + \mathbf{w}_k^{\mathbf{x}} \tag{2}$$

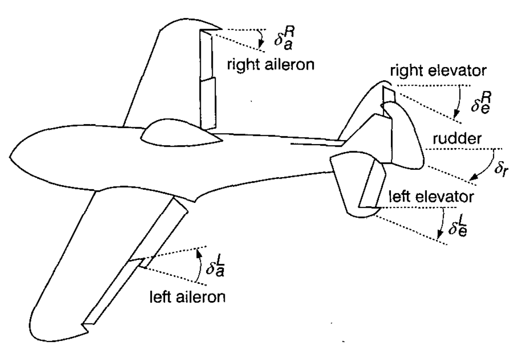

Fig. 2 *Control surfaces in an aircraft*

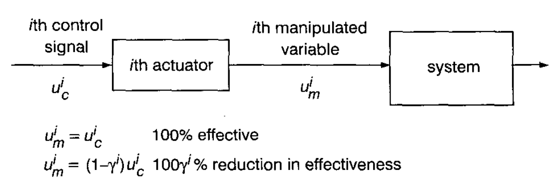

Fig. 3 *Modelling of actuator failures by control effectiveness factors*

where the post-fault control input matrix B_k^f relates to the nominal constant control input matrix B and the control effectiveness factors γ_k^i, $i = 1, \ldots, l$, in the following way

$$B_k^f = B(I - \Gamma_k), \quad \Gamma_k = \begin{bmatrix} \gamma_k^1 & 0 & \cdots & 0 \\ 0 & \gamma_k^2 & \ddots & 0 \\ \vdots & \ddots & \ddots & \vdots \\ 0 & 0 & \cdots & \gamma_k^l \end{bmatrix} \tag{3}$$

where $\gamma_k^i = 0$, $i = 1, \ldots, l$, denotes the healthy ith actuator and $\gamma_k^i = 1$ corresponds to total failure of the ith actuator. Naturally, $0 < \gamma_k^i < 1$ represents partial loss in control effectiveness. Due to the fact that the control effectiveness factors are parameters located between the controller command and the actuator actions, such modelling can be viewed as multiplicative faults in nature.

However, the above model is not suitable for direct estimation of the control effectiveness factors. An alternative representation of (2) is as follows

$$\mathbf{x}_{k+1} = A\mathbf{x}_k + B\mathbf{u}_k - [\mathbf{b}_1\gamma_k^1 \;\; \mathbf{b}_2\gamma_k^2 \;\; \ldots \;\; \mathbf{b}_l\gamma_k^l] \begin{bmatrix} u_k^1 \\ \vdots \\ u_k^l \end{bmatrix} + \mathbf{w}_k^x \tag{4}$$

or, more compactly

$$\mathbf{x}_{k+1} = A\mathbf{x}_k + B\mathbf{u}_k + D_k(\mathbf{u}_k)\gamma_k + \mathbf{w}_k^x \tag{5}$$

where $D_k(\mathbf{u}_k)$ is defined by

$$D_k(\mathbf{u}_k) \doteq BU_k \tag{6}$$

and

$$U_k = \begin{bmatrix} -u_k^1 & 0 & \cdots & 0 \\ 0 & -u_k^2 & \ddots & 0 \\ \vdots & \ddots & \ddots & \vdots \\ 0 & 0 & \cdots & -u_k^l \end{bmatrix}, \qquad \gamma_k = \begin{bmatrix} \gamma_k^1 \\ \gamma_k^2 \\ \vdots \\ \gamma_k^l \end{bmatrix} \tag{7}$$

The objective of FDD is to determine the extent of the loss in the control effectiveness, γ_k, so that an on-line automatic reconfigurable controller can be synthesised accordingly; therefore, the estimation of γ_k in a recursive form is highly desirable. In the absence of the knowledge of their true values, the control effectiveness factors can be modelled as a random bias vector:

$$\gamma_{k+1} = \gamma_k + \mathbf{w}_k^\gamma \begin{cases} \gamma_k = 0, k < k_F & \text{fault-free} \\ \gamma_k \neq 0, k \geq k_F & \text{with fault} \end{cases} \tag{8}$$

where k_F denotes unknown time instant when reduction of the control effectiveness occurred, $\mathbf{w}_k^\gamma$ is a zero-mean white Gaussian noise sequence with covariance Q_k^γ, and the initial state γ_0 is a Gaussian vector with mean $\bar{\gamma}_0$ and covariance P_0^γ.

Consequently, the combined state and control effectiveness model has the following form

$$\begin{aligned} \mathbf{x}_{k+1} &= A\mathbf{x}_k + B\mathbf{u}_k + D_k(\mathbf{u}_k)\gamma_k + \mathbf{w}_k^x \\ \gamma_{k+1} &= \gamma_k + \mathbf{w}_k^\gamma \qquad \begin{cases} \gamma_k = 0, k < k_F \\ \gamma_k \neq 0, k \geq k_F \end{cases} \\ \mathbf{y}_k &= C_r\mathbf{x}_k \\ \mathbf{z}_k &= C\mathbf{x}_k + \mathbf{v}_k \end{aligned} \tag{9}$$

Such actuator fault modelling has unique advantages over some existing techniques where only either normal or complete failure have been considered [11].

3 Fault detection, diagnosis and reconfiguration mechanism

3.1 Adaptive state and fault parameter estimation

To carry out on-line controller reconfiguration in the event of actuator failures, it is necessary to determine the control input matrix B_k^f in (2) on line. This matrix can be obtained through the estimated control effectiveness factors $\hat{\gamma}_k = [\hat{\gamma}_k^1 \; \hat{\gamma}_k^2 \cdots \hat{\gamma}_k^l]^T$ by

$$\hat{B}_k^f = B(I - \hat{\Gamma}_k) \tag{10}$$

where

$$\hat{\Gamma}_k = \begin{bmatrix} \bar{\hat{\gamma}}_k^1 & 0 & \cdots & 0 \\ 0 & \bar{\hat{\gamma}}_k^2 & \ddots & 0 \\ \vdots & \ddots & \ddots & \vdots \\ 0 & 0 & \cdots & \bar{\hat{\gamma}}_k^l \end{bmatrix} \tag{11}$$

and

$$\bar{\hat{\gamma}}_k^i = \sum_{j=k-N_A+1}^{k} \hat{\gamma}_j^i, \quad i = 1, \ldots, l; \quad k \geq k_D \tag{12}$$

where N_A is the length of the smoothing data window, and k_D is the time at which the fault has been detected. The purpose of the above moving window average for estimated $\hat{\gamma}_k$ is to reduce the model uncertainties in determining the post-fault system model.

To achieve reconfigurable control, both the system states and the control effectiveness factors are needed. One way to solve this problem is to estimate both $\mathbf{x}_k$ and γ_k [23]. This leads to a simultaneous state and parameter estimation problem. The structure of the filter is depicted in Fig. 4. A more detailed description of the filtering algorithm is represented in Table 1.

Remark: With the integrated FDD and reconfigurable control structure illustrated in Fig. 1, it is important to note that the input signal used in the filter is a closed-loop system signal, which is obtained at the controller output, i.e.

$$\mathbf{u}_k = K_{forward}\mathbf{r}_k + K_{feedback}\hat{\mathbf{x}}_{k|k} \tag{13}$$

3.2 Fault detection and isolation scheme

To perform fault detection and isolation, the following two-stage statistical hypothesis tests have been developed. In the first stage, the statistical quantities of the system under the normal operation, such as mean values and variances, are determined, and then the same quantities during the continuous system operation are calculated. By defining an appropriate statistical detection variable to accentuate the

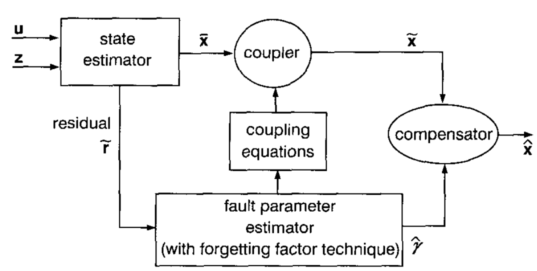

Fig. 4 *Simultaneous estimation of states and control effectiveness factors*

Table 1: Two-stage adaptive Kalman filtering algorithm

Consider the following system:

$$\mathbf{x}_{k+1} = A\mathbf{x}_k + B\mathbf{u}_k + D_k\gamma_k + \mathbf{w}_k^{\mathbf{x}}$$
$$\gamma_{k+1} = \gamma_k + \mathbf{w}_k^{\gamma}$$
$$\mathbf{z}_k = C\mathbf{x}_k + \mathbf{v}_k$$

with $\mathbf{w}_k^{\mathbf{x}} = \mathcal{N}[0, Q_k^{\mathbf{x}}]$; $\mathbf{w}_k^{\gamma} = \mathcal{N}[0, Q_k^{\gamma}]$; $\mathbf{v}_k = \mathcal{N}[0, R_k]$; $\bar{\mathbf{x}}_0 = \mathcal{N}[\bar{\mathbf{x}}_0, \bar{P}_0^{\mathbf{x}}]$; $\gamma_0 = \mathcal{N}[\bar{\gamma}_0, \bar{P}_0^{\gamma}]$

1. Control effectiveness factor estimator

$$\hat{\gamma}_{k+1|k} = \hat{\gamma}_{k|k}$$
$$P_{k+1|k}^{\gamma} = \sum_{i=1}^{l} \frac{1}{\rho_k^i} e_k^i \alpha_{k|k}^i (e_k^i)^T + Q_k^{\gamma}$$
$$\hat{\gamma}_{k+1|k+1} = \hat{\gamma}_{k+1|k} + L_{k+1}^{\gamma}(\tilde{\mathbf{r}}_{k+1} - H_{k+1|k}\hat{\gamma}_{k|k})$$
$$L_{k+1}^{\gamma} = P_{k+1|k}^{\gamma} H_{k+1|k}^T (H_{k+1|k} P_{k+1|k}^{\gamma} H_{k+1|k}^T + \tilde{S}_{k+1})^{-1}$$
$$P_{k+1|k+1}^{\gamma} = (I - L_{k+1}^{\gamma} H_{k+1|k}) P_{k+1|k}^{\gamma}$$

where

$$P_{k|k}^{\gamma} \triangleq \sum_{i=1}^{l} e_k^i \alpha_{k|k}^i (e_k^i)^T$$

$$\rho_k^i = \begin{cases} 1 & \alpha_{k|k}^i > \alpha_{\max} \\ \alpha_{k|k}^i \left[\alpha_{\min} + \dfrac{\alpha_{\max} - \alpha_{\min}}{\alpha_{\max}} \alpha_{k|k}^i\right]^{-1} & \alpha_{k|k}^i \le \alpha_{\max} \end{cases} \quad 0 < \rho_k^i \le 1$$

2. State estimator

$$\bar{x}_{k+1|k} = A\tilde{\mathbf{x}}_{k|k} + B\mathbf{u}_k$$
$$\tilde{\mathbf{x}}_{k+1|k} = \bar{\mathbf{x}}_{k+1|k} + W_k \hat{\gamma}_{k|k} - V_{k+1|k}\hat{\gamma}_{k|k}$$
$$\bar{P}_{k+1|k}^{\mathbf{x}} = A\tilde{P}_{k|k}^{\mathbf{x}} A^T + Q_k^{\mathbf{x}}$$
$$\tilde{P}_{k+1|k}^{\mathbf{x}} = \bar{P}_{k+1|k}^{\mathbf{x}} + W_k P_{k|k}^{\gamma} W_k^T - V_{k+1|k} P_{k+1|k}^{\gamma} V_{k+1|k}^T$$
$$\tilde{\mathbf{x}}_{k+1|k+1} = \tilde{\mathbf{x}}_{k+1|k} + \tilde{L}_{k+1}^{\mathbf{x}}(\mathbf{z}_{k+1} - C\tilde{\mathbf{x}}_{k+1|k})$$
$$\tilde{L}_{k+1}^{\mathbf{x}} = \tilde{P}_{k+1|k}^{\mathbf{x}} C^T (C\tilde{P}_{k+1|k}^{\mathbf{x}} C^T + R_{k+1})^{-1}$$
$$\tilde{P}_{k+1|k+1}^{\mathbf{x}} = (I - \tilde{L}_{k+1}^{\mathbf{x}} C)\tilde{P}_{k+1|k}^{\mathbf{x}}$$

where the residual vector and its covariance matrix are given as

$$\tilde{\mathbf{r}}_{k+1} = \mathbf{z}_{k+1} - C\tilde{\mathbf{x}}_{k+1|k}$$
$$\tilde{S}_{k+1} = C\tilde{P}_{k+1|k}^{\mathbf{x}} C^T + R_{k+1}$$

3. Coupling equations

$$W_k = AV_{k|k} + D_k$$
$$V_{k+1|k} = W_k P_{k|k}^{\gamma} (P_{k+1|k}^{\gamma})^{-1}$$
$$H_{k+1|k} = CV_{k+1|k}$$
$$V_{k+1|k+1} = V_{k+1|k} - \tilde{L}_{k+1}^{\mathbf{x}} H_{k+1|k}$$

4. Compensated state and error covariance estimates

$$\hat{\mathbf{x}}_{k+1|k+1} = \tilde{\mathbf{x}}_{k+1|k+1} + V_{k+1|k+1}\hat{\gamma}_{k+1|k+1}$$
$$P_{k+1|k+1} = \tilde{P}_{k+1|k+1}^{\mathbf{x}} + V_{k+1|k+1} P_{k+1|k+1}^{\gamma} V_{k+1|k+1}^T$$

deviation in the statistical quantities from their normal values, the detection and isolation of the reduction of control effectiveness can be achieved recursively.

Stage 1: Under the normal condition we have

$$\hat{\gamma}_k \sim \mathcal{N}(\bar{\boldsymbol{\mu}}_{\hat{\gamma}_0}, \boldsymbol{\sigma}_{\hat{\gamma}_0}^2) \tag{14}$$

where $\hat{\gamma}_k \in \Re^l$ is the estimate of the reduction of control effectiveness, which can also be used as the residual vector for fault detection, and $\bar{\boldsymbol{\mu}}_{\hat{\gamma}_0} = [\bar{\mu}_{\hat{\gamma}_0^1}\ \bar{\mu}_{\hat{\gamma}_0^2}\ \cdots\ \bar{\mu}_{\hat{\gamma}_0^l}]^T$ and $\boldsymbol{\sigma}_{\hat{\gamma}_0}^2 = \mathrm{diag}[\sigma_{\hat{\gamma}_0^1}^2\ \sigma_{\hat{\gamma}_0^2}^2\ \cdots\ \sigma_{\hat{\gamma}_0^l}^2]$ are the mean and variance, respectively. These values are obtained for $i = 1, \ldots, l$ from

$$\bar{\mu}_{\hat{\gamma}_0^i} = \frac{1}{N_1}\sum_{j=1}^{N_1} \hat{\gamma}_j^i \tag{15}$$

$$\sigma_{\hat{\gamma}_0^i}^2 = \frac{1}{N_1 - 1}\sum_{j=1}^{N_1} [\hat{\gamma}_j^i - \bar{\mu}_{\hat{\gamma}_0^i}]^2 \tag{16}$$

The sample size N_1 is chosen to ensure the sufficiency in statistics.

Stage 2: Define the following moving window based statistical quantities:

$$\bar{\mu}_{\hat{\gamma}_k^i} = \frac{1}{N_2}\sum_{j=k-N_2+1}^{k} \hat{\gamma}_j^i = \bar{\mu}_{\hat{\gamma}_{k-1}^i} - \frac{1}{N_2}[\hat{\gamma}_{k-N_2}^i - \hat{\gamma}_k^i] \tag{17}$$

$$\sigma_{\hat{\gamma}_k^i I}^2 = \frac{1}{N_2 - 1}\sum_{j=k-N_2+1}^{k} [\hat{\gamma}_j^i - \bar{\mu}_{\hat{\gamma}_0^i}]^2 = \sigma_{\hat{\gamma}_{k-1}^i I}^2 - \frac{1}{N_2 - 1}\left[(\hat{\gamma}_{k-N_2}^i)^2 - (\hat{\gamma}_k^i)^2 - 2\bar{\mu}_{\hat{\gamma}_0^i}\varepsilon_k^i\right] \tag{18}$$

$$\sigma_{\hat{\gamma}_k^i II}^2 = \frac{1}{N_2 - 1}\sum_{j=k-N_2+1}^{k} [\hat{\gamma}_j^i - \bar{\mu}_{\hat{\gamma}_k^i}]^2 = \sigma_{\hat{\gamma}_{k-1}^i II}^2 + \frac{1}{N_2 - 1}\left[2\varepsilon_k^i\bar{\mu}_{\hat{\gamma}_{k-1}^i} - (\hat{\gamma}_{k-N_2}^i)^2 + (\hat{\gamma}_k^i)^2 - \frac{1}{N_2 - 1}(\varepsilon_k^i)^2\right] \tag{19}$$

where $\varepsilon_k^i = \hat{\gamma}_{k-N_2}^i - \hat{\gamma}_k^i$ and N_2 is the length of the moving window.

Consequently, a fault in the ith actuator is declared at time k if the following detection index

$$d_k^i = \frac{\sigma^2_{\hat{\gamma}_k^i I}}{\sigma^2_{\hat{\gamma}_0^i}} - \ln \frac{\sigma^2_{\hat{\gamma}_k^i II}}{\sigma^2_{\hat{\gamma}_0^i}} - 1, \quad i = 1, \ldots, l \tag{20}$$

exceeds a preset threshold η^i.

$$d_k^i \underset{H_0}{\overset{H_i}{\gtrless}} \eta^i \tag{21}$$

where $H_0 = \{$no significant reduction in the effectiveness of the ith actuator$\}$, $H_i = \{$there is significant reduction in the effectiveness of the ith actuator$\}$. Here, 'significant reduction' is a design parameter and should be reflected in the selection of the threshold η^i. The selection of the window length, N_2, and the threshold, η^i, represents some trade-off between the probability of false alarm and the probability of missed detection.

3.3 Activation of reconfiguration process

Once the fault is declared, to design an effective reconfigurable control system, the accurate estimation of the reduction of the control effectiveness is required to form the new control input matrix $\hat{B}_k^f$ in (10). Since it is important to design reconfigurable control laws based on the accurate parameter estimates, the activation of the reconfiguration process should only take place when the consecutive fault parameter estimates satisfy the following smooth condition:

$$r_k^i = |\hat{\gamma}_k^i - \hat{\gamma}_{k-1}^i| < \delta^i, \ \forall i = 1, \ldots, l; \quad k \geq k_D \tag{22}$$

The threshold δ^i is also a design parameter. The time instant at which the above threshold is exceeded for the first time is referred to as the controller reconfiguration time, k_R.

4 Design of reconfigurable feedback and feedforward controllers

Eigenstructure assignment (EA) and the linear quadratic regulator (LQR) are among the most popular controller design techniques for multi-input and multi-output systems. The advantage of EA is that if the specifications are given in terms of the system eigenstructure, the eigenstructure can be achieved exactly for the desired stability and dynamic performance. Therefore, EA is used for the reconfigurable control system design. Fig. 5 shows the configuration of the proposed integrated FDD and reconfigurable control scheme.

4.1 Reconfigurable feedback control design via eigenstructure assignment

Since the stability and the dynamic behaviour of a closed-loop system is governed by its eigenstructure, in the context of fault-tolerant control, to recover the performance of the pre-fault system, the eigenstructure of the reconfigured system should be as close to that of the pre-fault system as possible.

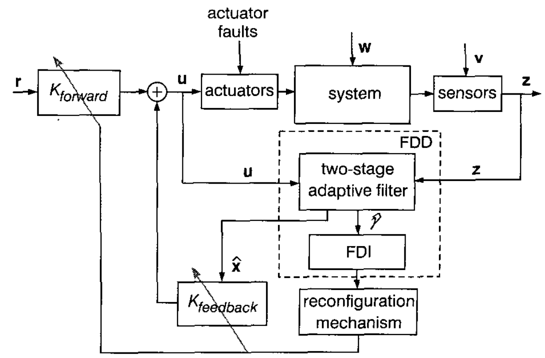

Fig. 5 *Integrated FDD and reconfigurable control configuration*

4.1.1 Desirable eigenvalues and eigenvectors: Due to the reduction of the control effectiveness, the system with actuator faults has become

$$\mathbf{x}_{k+1} = A\mathbf{x}_k + \hat{B}_k^f \mathbf{u}_k + \mathbf{w}_k^{\mathbf{x}}$$

The first objective of the reconfigurable control system design is to synthesise a feedback controller so that

$$\lambda_i^f = \lambda(A + \hat{B}_k^f K_{feedback}) = \lambda_i = \lambda(A + BK_{normal}), \quad i = 1, \ldots, n \tag{23}$$

where K_{normal} is the feedback control gain matrix in the fault-free system, and $K_{feedback}$ represents the desired new feedback control gain matrix. $\lambda(\cdot)$ denotes the eigenvalues of the system.

By definition, the closed-loop eigenvectors of the reconfigured system, $\{\mathbf{v}_i^f, i = 1, \ldots, n\}$, will satisfy

$$(A + \hat{B}_k^f K_{feedback})\mathbf{v}_i^f = \lambda_i^f \mathbf{v}_i^f \tag{24}$$

or

$$\mathbf{v}_i^f = \underbrace{(\lambda_i^f I - A)^{-1}\hat{B}_k^f}_{E_i} \underbrace{K_{feedback}\mathbf{v}_i^f}_{\mathbf{w}_i} \tag{25}$$

The other objective is to synthesise the feedback gain matrix $K_{feedback}$ such that the closed-loop eigenvectors of the reconfigured system $\mathbf{v}_i^f$ are as close to the corresponding eigenvectors of the pre-fault system $\mathbf{v}_i$ as possible. Because of the variations in system dynamics due to the faults, in general, $\mathbf{v}_i^f$ does not lie in the same subspace as $\mathbf{v}_i$. However, a 'best possible' choice for an achievable eigenvector $\mathbf{v}_i^f$ can be obtained by projecting the desired eigenvector $\mathbf{v}_i$ onto the subspace spanned by the columns of $E_i = (\lambda_i^f I - A)^{-1}\hat{B}_k^f$. Then, (25) can be rewritten as

$$\mathbf{v}_i^f = E_i \mathbf{w}_i \tag{26}$$

where

$$\mathbf{w}_i = K_{feedback}\mathbf{v}_i^f \tag{27}$$

To determine $\mathbf{v}_i^f$ by projecting $\mathbf{v}_i$ onto the achievable subspace, the following least squares minimisation procedure is employed

$$\begin{aligned} \min J_i(\mathbf{v}_i^f) &= \min\{(\mathbf{v}_i^f - \mathbf{v}_i)^T W_i (\mathbf{v}_i^f - \mathbf{v}_i)\} \\ &= \min\{(E_i\mathbf{w}_i - \mathbf{v}_i)^T W_i (E_i\mathbf{w}_i - \mathbf{v}_i)\}, \quad i = 1, \ldots, n \end{aligned} \tag{28}$$

The solution to this optimisation leads to

$$\mathbf{w}_i = (E_i^T W_i^T W_i E_i)^{-1} E_i^T W_i^T \mathbf{v}_i \tag{29}$$

Substituting (29) into (26), the most desirable closed-loop eigenvector $\mathbf{v}_i^f$ is given as

$$\mathbf{v}_i^f = E_i(E_i^T W_i^T W_i E_i)^{-1} E_i^T W_i^T \mathbf{v}_i \quad (30)$$

where $W_i \in \Re^{n\times n}$ is a positive definite weighting matrix. Suggestions about how to choose the weighting matrix W_i are given in [17]. The solution to this projection problem exists as long as the eigenvalues of the closed-loop system are different from those of the open-loop system.

4.1.2 Calculation of reconfigurable control gain matrix: Consider the following equation describing the closed-loop reconfigured system

$$\mathbf{x}_{k+1} = (A + \hat{B}_k^f K_{feedback})\mathbf{x}_k \quad (31)$$

To simplify the procedure in calculating the matrix $K_{feedback}$, a linear transformation matrix

$$\Omega = [\hat{B}_k^f \vdots \Theta] \in \Re^{n\times n} \quad (32)$$

is chosen, where $\Theta \in \Re^{n\times(n-l)}$ is an arbitrary matrix such that $\mathrm{rank}(\Omega) = n$.

Applying Ω to (31) will lead to a new set of state variables $\bar{\mathbf{x}}_k \in \Re^n$:

$$\bar{\mathbf{x}}_k = \Omega^{-1}\mathbf{x}_k \quad (33)$$

Thus (31) becomes:

$$\bar{\mathbf{x}}_{k+1} = (\bar{A} + \bar{B}_k^f K_{feedback}\Omega)\bar{\mathbf{x}}_k \quad (34)$$

where $\bar{A} = \Omega^{-1}A\Omega$ and $\bar{B}_k^f = \Omega^{-1}\hat{B}_k^f = [I_l/0]$. The corresponding eigenvectors are related by $\bar{\mathbf{v}}_i^f = \Omega^{-1}\mathbf{v}_i^f = [\mathbf{s}_i/\mathbf{g}_i]$.

Clearly, the eigenvalues, eigenvectors and the system matrices will satisfy

$$(\bar{A} + \bar{B}_k^f K_{feedback}\Omega)\bar{\mathbf{v}}_i^f = \lambda_i^f \bar{\mathbf{v}}_i^f, \quad i = 1, \ldots, n \quad (35)$$

(35) can be rearranged as

$$(\lambda_i^f I - \bar{A})\bar{\mathbf{v}}_i^f = \bar{B}_k^f K_{feedback}\Omega\bar{\mathbf{v}}_i^f, \quad i = 1, \ldots, n \quad (36)$$

From the special structure of $\bar{B}_k^f$, (36) becomes:

$$\left[\begin{array}{c|c} \lambda_i^f I_l - \bar{A}_{11} & -\bar{A}_{12} \\ \hline -\bar{A}_{21} & \lambda_i^f I_{n-l} - \bar{A}_{22} \end{array}\right]\begin{bmatrix} \mathbf{s}_i \\ \mathbf{g}_i \end{bmatrix} = \begin{bmatrix} I_l \\ 0 \end{bmatrix} K_{feedback}\Omega\begin{bmatrix} \mathbf{s}_i \\ \mathbf{g}_i \end{bmatrix} \quad (37)$$

where

$$\bar{A} = \left[\begin{array}{c|c} \bar{A}_{11} & \bar{A}_{12} \\ \hline \bar{A}_{21} & \bar{A}_{22} \end{array}\right] = \Omega^{-1}A\Omega$$

The first matrix equation in the partitioned form can be written as

$$(\lambda_i^f I_l - \bar{A}_{11})\mathbf{s}_i - \bar{A}_{12}\mathbf{g}_i = K_{feedback}\Omega\begin{bmatrix} \mathbf{s}_i \\ \mathbf{g}_i \end{bmatrix} \quad i = 1, \ldots, n \quad (38)$$

Further, by letting

$$\bar{A}_1 = \begin{bmatrix} \bar{A}_{11} & \bar{A}_{12} \end{bmatrix}$$

(38) becomes

$$[\bar{A}_1 + K_{feedback}\Omega]\bar{\mathbf{v}}_i^f = \lambda_i^f \mathbf{s}_i, \quad i = 1, \ldots, n \quad (39)$$

or, in a compact form

$$[\bar{A}_1 + K_{feedback}\Omega]\bar{V}_f = S \quad (40)$$

where $\bar{V}_f = [\bar{\mathbf{v}}_1^f \; \bar{\mathbf{v}}_2^f \; \cdots \; \bar{\mathbf{v}}_n^f] \in \mathfrak{C}^{n\times n}$, and $S = [\lambda_1^f \mathbf{s}_1 \; \lambda_2^f \mathbf{s}_2 \; \cdots \; \lambda_n^f \mathbf{s}_n] \in \mathfrak{C}^{l\times n}$.

Finally, the desired feedback gain matrix can be obtained as follows:

$$K_{feedback} = (S - \bar{A}_1\bar{V}_f)(\Omega\bar{V}_f)^{-1} \quad (41)$$

4.2 Reconfigurable feedforward controller

Since the feedback control can only guarantee the dynamic behaviour of the system, a reconfigurable feedforward controller is needed to achieve steady-state tracking of the reference input. For this reason, a feedforward control law based on a command generator tracker (CGT) [24, 25] is developed in this paper for discrete systems. The basic principle of the CGT is to make the system outputs to track the command inputs via proper design of a feedforward controller based on the model-following principle.

For the system described in (1) and (2), suppose that the desired behaviour of a plant is described by

$$\begin{aligned} \mathbf{x}_{k+1}^m &= A^m\mathbf{x}_k^m + B^m\mathbf{r}_k \\ \mathbf{y}_k^m &= C^m\mathbf{x}_k^m + D^m\mathbf{r}_k \end{aligned} \quad (42)$$

where $\mathbf{x}_k^m \in \Re^{n^m}$, $\mathbf{r}_k \in \Re^{l^m}$ and $\mathbf{y}_k^m \in \Re^{p^m}$.

The problem of determining the solution for perfect tracking can be formulated as follows: find a control sequence $\mathbf{u}_k$ that forces the command tracking error $\mathbf{e}_k$ to zero for all $k > 0$, if $\mathbf{e}_0 = 0$.

$$\mathbf{e}_k = \mathbf{y}_k - \mathbf{y}_k^m = \begin{bmatrix} C_r & 0 \end{bmatrix}\begin{bmatrix} \mathbf{x}_k \\ \mathbf{u}_k \end{bmatrix} - \begin{bmatrix} C^m & D^m \end{bmatrix}\begin{bmatrix} \mathbf{x}_k^m \\ \mathbf{r}_k \end{bmatrix} = 0 \quad (43)$$

where the matrix C_r is chosen so that

$$\mathbf{r}_k = \mathbf{y}_k = C_r\mathbf{x}_k \quad (44)$$

The condition under which the command tracking error approaches zero asymptotically will be called perfect tracking. If the resulting system state and control trajectories are denoted by $\mathbf{x}_k^*$ and $\mathbf{u}_k^*$, then, $\mathbf{x}_k^*$ and $\mathbf{u}_k^*$ will satisfy

$$\mathbf{y}_k^* = \begin{bmatrix} C_r & 0 \end{bmatrix}\begin{bmatrix} \mathbf{x}_k^* \\ \mathbf{u}_k^* \end{bmatrix} = \begin{bmatrix} C^m & D^m \end{bmatrix}\begin{bmatrix} \mathbf{x}_k^m \\ \mathbf{r}_k \end{bmatrix} \quad (45)$$

and the plant dynamics

$$\mathbf{x}_{k+1}^* = A\mathbf{x}_k^* + B\mathbf{u}_k^* \quad (46)$$

If the signal to be tracked is the command input, the above reference model can be chosen as an identity model, i.e.

$$\mathbf{y}_k^m = \mathbf{r}_k \quad (47)$$

therefore, the identity model can be described by

$$A^m = I, \; B^m = 0, \; C^m = 0, \; D^m = I \quad (48)$$

With the assumption [25] that the ideal plant state $\mathbf{x}_k^*$ and control trajectories $\mathbf{u}_k^*$ are linear combinations of the states and inputs of the reference model as follows:

$$\mathbf{x}_k^* = S_{11}\mathbf{x}_k^m + S_{12}\mathbf{r}_k + O(\mathbf{r}_k) \quad (49)$$

$$\mathbf{u}_k^* = S_{21}\mathbf{x}_k^m + S_{22}\mathbf{r}_k + O(\mathbf{r}_k) \quad (50)$$

where S_{ij} are constant feedforward gain matrices, if we restrict $\mathbf{r}_k$ to step inputs, then $O(\mathbf{r}_k) = 0$ for all $k > k_0$. In this case, the perfect tracking problem becomes one of determining solvable expressions for all S_{ij} matrices based on the identity model given in (48). The solution for the plant state $\mathbf{x}_k^*$ and the control input $\mathbf{u}_k^*$ can be found as

$$\mathbf{x}_k^* = \Phi_{12}\mathbf{r}_k \tag{51}$$

$$\mathbf{u}_k^* = \Phi_{22}\mathbf{r}_k \tag{52}$$

where $S_{12} = \Phi_{12}$, $S_{22} = \Phi_{22}$ and Φ_{ij} are given by

$$\Phi = \begin{bmatrix} \Phi_{11} & \Phi_{12} \\ \Phi_{21} & \Phi_{22} \end{bmatrix} = \begin{cases} \begin{bmatrix} A - I & B \\ C_r & 0 \end{bmatrix}^{-1} & \text{fault-free} \\ \begin{bmatrix} A - I & \hat{B}_k^f \\ C_r & 0 \end{bmatrix}^{-1} & \text{with fault} \end{cases} \tag{53}$$

To incorporate the feedback into the design, define

$$\tilde{\mathbf{x}}_k = \mathbf{x}_k - \mathbf{x}_k^*, \quad \tilde{\mathbf{u}}_k = \mathbf{u}_k - \mathbf{u}_k^*, \quad \tilde{\mathbf{y}}_k = \mathbf{y}_k - \mathbf{y}_k^* \tag{54}$$

then:

$$\tilde{\mathbf{x}}_{k+1} = \begin{cases} A\tilde{\mathbf{x}}_k + B\tilde{\mathbf{u}}_k & \text{fault-free} \\ A\tilde{\mathbf{x}}_k + \hat{B}_k^f\tilde{\mathbf{u}}_k & \text{with fault} \end{cases} \tag{55}$$

The state feedback control law for (55) is given by

$$\tilde{\mathbf{u}}_k = K_{feedback}\tilde{\mathbf{x}}_k = K_{feedback}(\mathbf{x}_k - \mathbf{x}_k^*) \tag{56}$$

From the definition of $\tilde{\mathbf{u}}_k$ in (54) and combining with (56):

$$\mathbf{u}_k = \mathbf{u}_k^* + \tilde{\mathbf{u}}_k = \mathbf{u}_k^* + K_{feedback}(\mathbf{x}_k - \mathbf{x}_k^*) \tag{57}$$

Substituting (51) and (52) into (57), we have

$$\mathbf{u}_k = \underbrace{(\Phi_{22} - K_{feedback}\Phi_{12})\mathbf{r}_k}_{\text{feedforward}} + \underbrace{K_{feedback}\mathbf{x}_k}_{\text{feedback}} \tag{58}$$

Note that this control law consists of a feedback part and a feedforward part. The feedforward part is a function of the feedback gain matrix.

5 Simulation example and performance evaluation

The effectiveness of the proposed scheme is demonstrated in this Section through a longitudinal vertical takeoff and landing (VTOL) aircraft model [26].

5.1 Simulation example

The linearised model of the aircraft for a typical loading and flight condition at an airspeed of 135 knots can be described as

$$\begin{aligned} \dot{\mathbf{x}}(t) &= A_c\mathbf{x}(t) + B_c\mathbf{u}(t) \\ \mathbf{z}(t) &= C_c\mathbf{x}(t) \end{aligned} \tag{59}$$

where $\mathbf{x} = [u\ v\ q\ \theta]^T$, $\mathbf{u} = [\delta_c\ \delta_l]^T$. The states are: horizontal velocity, u, vertical velocity, v, pitch rate, q, and pitch angle, θ; the control inputs are: blade angle of collective pitch control, δ_c, and blade angle of longitudinal cyclic pitch control, δ_l, where the collective pitch control is achieved by changing the pitch angle of all the main rotor blades by the same amount (collectively) through a hydraulically-driven actuation system. This includes mechanical linkages, hydraulic drivers, the rotors, as well as the coupling to achieve the blade angle adjustment, and the cyclic pitch control is achieved by changing the pitch angle of the tail rotor blades individually to cause a pitching moment to the aircraft. Any abnormal operations among any of the above elements are considered as actuator faults, which could prevent the control commands from executing perfectly at their manipulated variables, i.e. the pitch angles of the blades. Under the normal flight condition, the matrices A_c, B_c and C_c are given as follows:

$$A_c = \begin{bmatrix} -0.0366 & 0.0271 & 0.0188 & -0.4555 \\ 0.0482 & -1.01 & 0.0024 & -4.0208 \\ 0.1002 & 0.3681 & -0.707 & 1.420 \\ 0.0 & 0.0 & 1.0 & 0.0 \end{bmatrix}$$

$$B_c = \begin{bmatrix} 0.4422 & 0.1761 \\ 3.5446 & -7.5922 \\ -5.52 & 4.49 \\ 0.0 & 0.0 \end{bmatrix}$$

$$C_c = \begin{bmatrix} 1 & 0 & 0 & 0 \\ 0 & 1 & 0 & 0 \\ 0 & 0 & 1 & 0 \\ 0 & 1 & 1 & 1 \end{bmatrix}$$

Taking into consideration possible random noise in the system and representing the system in the discrete domain, we have:

$$\begin{aligned} \mathbf{x}_{k+1} &= A\mathbf{x}_k + B\mathbf{u}_k + \mathbf{w}_k^{\mathbf{x}} \\ \mathbf{z}_{k+1} &= C\mathbf{x}_{k+1} + \mathbf{v}_{k+1} \end{aligned} \tag{60}$$

where the sampling period $T = 0.1$ s is used, and $A = e^{A_cT}$, $B = (\int_0^T e^{A_c\tau}\, d\tau)B_c$, $C = C_c$.

Parameters used in the simulation are as follows. $Q^x = \text{diag}\{0.01^2,\ 0.01^2,\ 0.01^2,\ 0.01^2\}$, $Q^y = \text{diag}\{0.001^2,\ 0.001^2\}$, $R = \text{diag}\{0.1^2,\ 0.1^2\}$, $\mathbf{x}_0 = [20\ \ 10\ \ 8\ \ 1]^T$, $\gamma_0 = [0\ \ 0]^T$. Initial parameters of the two-stage Kalman filter are $\tilde{\mathbf{x}}_0 = \mathbf{x}_0$, $\hat{\gamma}_0 = \gamma_0$, $\tilde{P}_0^x = 10I$, $P_0^\gamma = 10I$, $Q_k^x = Q^x$, $Q_k^\gamma = Q^\gamma$, and $R_k = R$. C_r is chosen as

$$C_r = \begin{bmatrix} 1 & 0 & 0 & 0 \\ 0 & 1 & 0 & 0 \end{bmatrix}$$

5.2 Fault scenarios and reference inputs

The performance of the FDD and reconfigurable controller depend, to some extent, on the test scenarios used. In order to achieve a fair evaluation, several test scenarios for different types of fault and reference input have been considered.

5.2.1 Fault scenarios: To simulate different types of actuator impairment, five comprehensively designed fault scenarios were used, as shown in Table 2. These scenarios include reduction of the control effectiveness in a single actuator (scenario 1), asynchronous reductions of the control effectiveness in both actuators (scenario 2), gradual reduction in one actuator followed by an abrupt reduction in the other actuator (scenario 3), two consecutive reductions in one actuator followed by a reduction in the second actuator (scenario 4), and gradual reduction followed by abrupt reduction in one actuator, and then by another reduction in the second actuator (scenario 5). The design of such complex test scenarios is to ensure that the performance of the proposed scheme is evaluated as completely as possible.

Table 2: Test fault scenarios

Scenarios	Reduction of control effectiveness	k_F, s: 0	5	10	12.5
1	actuator 1	0%	0%	0%	0%
	actuator 2	0%	75%	75%	75%
2	actuator 1	0%	95%	95%	95%
	actuator 2	0%	0%	75%	75%
3	actuator 1	0%	$0 \rightarrow 95^{gradual}$%		95%
	actuator 2	0%	0%	0%	75%
4	actuator 1	0%	50%	95%	95%
	actuator 2	0%	0%	0%	75%
5	actuator 1	0%	$50 \rightarrow 95^{gradual}$%		95%
	actuator 2	0%	0%	0%	75%

5.2.2 Reference inputs: To demonstrate the effectiveness of the proposed scheme for tracking different reference inputs even in the presence of actuator faults, three types of reference input have been considered: (i) constant, (ii) constant with abrupt and incipient changes, and (iii) arbitrarily varying inputs.

5.3 Simulation results and performance evaluation

5.3.1 Constant reference inputs: Fig. 6 presents the outputs of the proposed scheme under the conditions of a constant reference input $\mathbf{r}_k = [5\ 5]^T$ and in test scenario 2. In scenario 2, consecutive partial actuator faults have been considered, where a 95% reduction of control effectiveness in the first actuator and a 75% reduction of control effectiveness in the second actuator occurred at $k = 5$ s and $k = 10$ s, respectively. For comparison purposes, the system outputs if there were no fault and the ones without the controller reconfiguration are also presented.

As can be seen, both the dynamic and steady-state performance of the system have been completely recovered with reasonably small transients. The outputs of the reconfigured system track the reference input even in the presence of the faults. Without reconfiguration, however, the performance of the closed-loop system becomes totally unacceptable.

For any FDD and reconfigurable FTCS there are detection and reconfiguration delays. It is highly desirable in FTCS to reduce these delays as much as possible. Using the developed integrated FTCS design the detection and reconfiguration delays are small. The detection and reconfiguration times are listed in Table 3.

Fig. 7 presents the time history of the detection index. The estimation of the reduction of control effectiveness for the two actuators is shown in Fig. 8. Note that the estimation is represented by the percentage in the reduction of the control effectiveness. It can be seen that prompt and accurate estimation have been obtained. Fig. 9 demonstrates the time history of the closed-loop control signals, from which one can easily see how the closed-loop control signals have changed automatically to compensate for the faults.

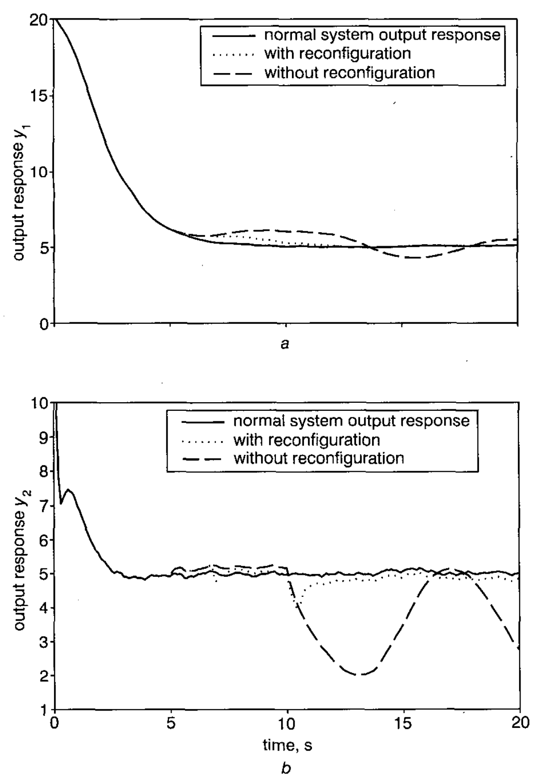

Fig. 6 *Output responses for scenario 2*
a Output response y_1
b Output response y_2

5.3.2 Time-varying reference inputs: To show the ability of the proposed scheme to recover the pre-fault performance even with an arbitrarily varying reference input, the results of scenario 3 are illustrated in Figs. 10 and 11. The reason for selecting scenario 3 is to show the system performance under more complicated fault situations, where both abrupt and incipient faults, and both single and multiple faults, have been simulated. It can be observed that satisfactory FDD and reconfiguration performance have also been obtained in this case. Without reconfiguration, however, the system performance is completely unacceptable.

Table 3: Detection and reconfiguration time

Actuator number	k_F, s	k_D, s	k_R, s
1	5.0	5.4	5.4
2	10.0	10.3	10.7

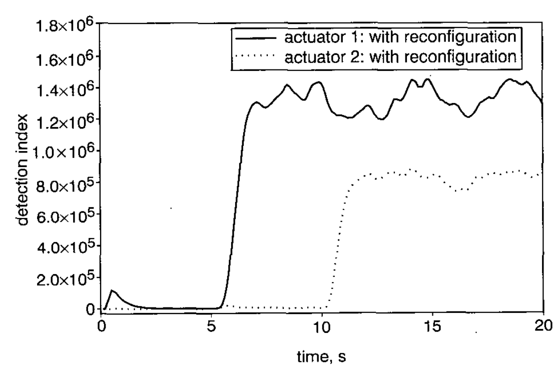

Fig. 7 *Detection index for scenario 2*

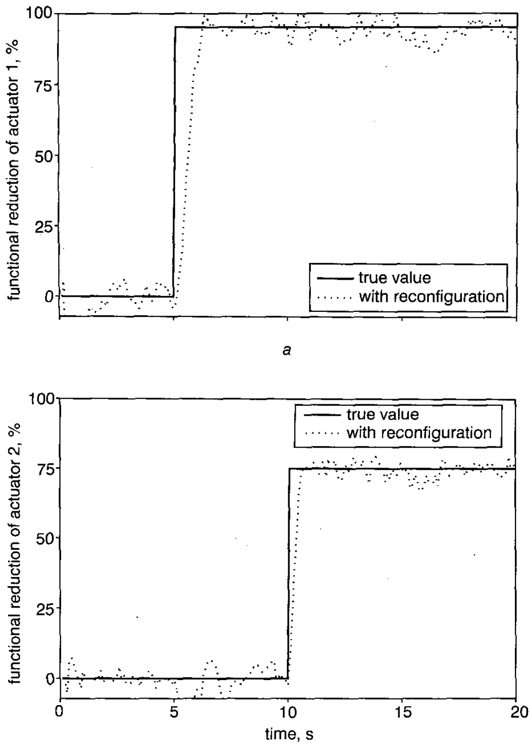

Fig. 8 *Fault estimates for scenario 2*

a Functional reduction of actuator 1
b Functional reduction of actuator 2

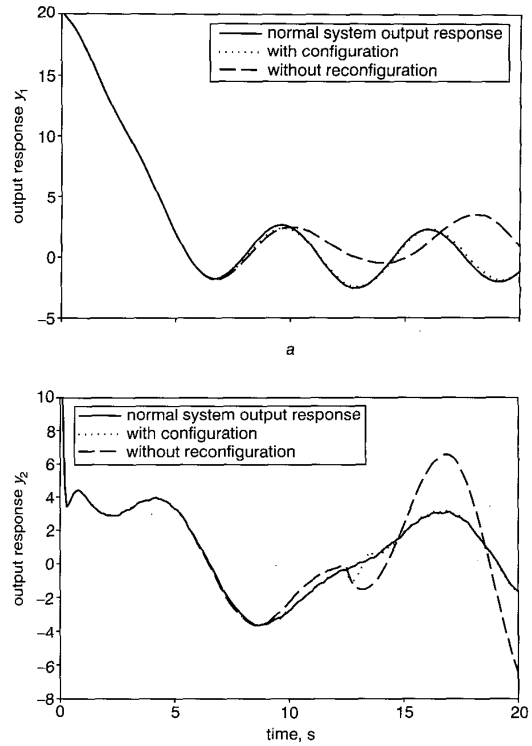

Fig. 10 *Output responses for scenario 3*

a Output response y_1
b Output response y_2

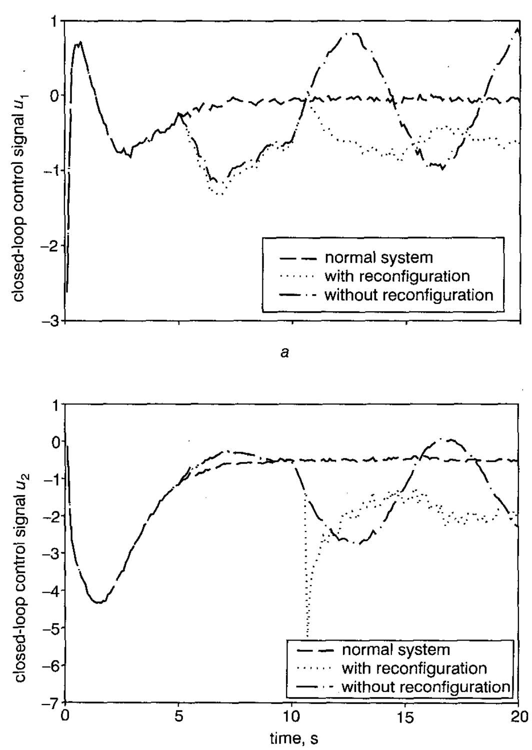

Fig. 9 *Closed-loop control signals for scenario 2*

a Closed-loop control signal u_1
b Closed-loop control signal u_2

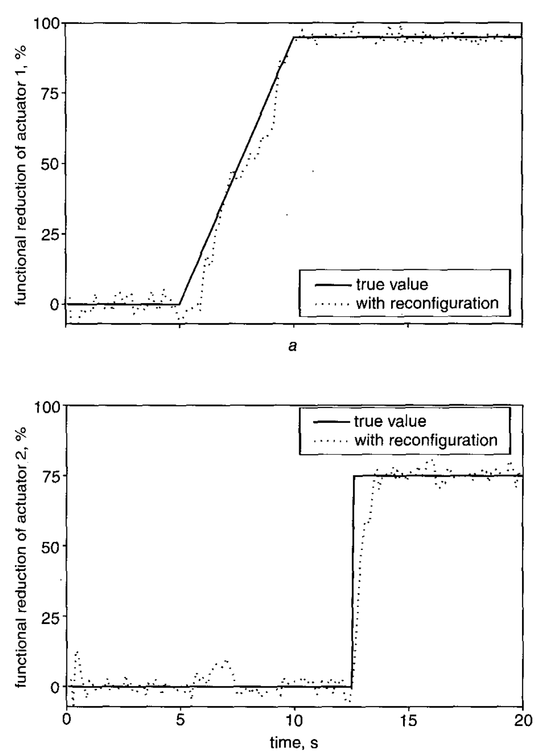

Fig. 11 *Fault estimates for scenario 3*

a Functional reduction of actuator 1
b Functional reduction of actuator 2

6 Conclusions and comments

An integrated fault detection, diagnosis and reconfigurable control system design approach in the framework of discrete-time stochastic systems has been proposed in this paper. The proposed scheme is based on a two-stage adaptive Kalman filter for the state and fault parameter estimation, the robust statistical decisions for fault detection, diagnosis and activation of the controller reconfiguration, and an on-line reconfigurable feedback control law synthesis based on an eigenstructure assignment technique. Effective tracking of the reference input has been achieved using the command generator tracker with a reconfigurable feedforward control law. Simulation results have demonstrated the effectiveness of the proposed technique.

It should be pointed out that an alternative way to achieve command tracking is to use a proportional-integral (PI) control structure [12]. Compared with the PI controller, in addition to its simpler structure, the feedforward control offers faster reaction and smoother response in the event of the fault, and it has the ability to completely reject any known disturbances. In this paper, only actuator faults have been considered, although the scheme could be extended to deal with sensor and system component faults, as long as all fault parameters can be represented by a bias vector γ_k, which can then be estimated by the two-stage adaptive Kalman filter.

7 Acknowledgments

This project was partially supported by the Natural Sciences and Engineering Research Council of Canada.

8 References

1 BASSEVILLE, M.: 'Detecting changes in signals and systems—a survey', *Automatica*, 1988, **24**, (3), pp. 309–326
2 ISERMANN, R.: 'Special section of papers on supervision, fault detection and diagnosis of technical systems', *Control Eng. Pract.*, 1997, **5**, (5), pp. 637–719
3 FRANK, P.M.: 'Fault diagnosis in dynamic systems using analytical and knowledge-based redundancy—a survey and some new results', *Automatica*, 1990, **26**, (3), pp. 459–474
4 GERTLER, J.: 'Survey of model-based failure detection and isolation in complex plants', *IEEE Control Syst. Mag.*, 1988, **8**, (6), pp. 3–11
5 PATTON, R.J., FRANK, P.M., and CLARK, R.N.: 'Fault diagnosis in dynamic systems, theory and applications' (Prentice-Hall, Englewood Cliffs, NJ, 1989)
6 WILLSKY, A.S.: 'A survey of design methods for failure detection in dynamic systems', *Automatica*, 1976, **12**, (6), pp. 601–611
7 CHANDLER, P.R.: 'Self-repairing flight control system reliability and maintainability program executive overview'. Proceedings of IEEE national aerospace and electronics conference, 1984, Dayton, OH, pp. 586–590
8 LOOZE, D.P., WEISS, J.L., ETERNO, J.S., and BARRETT, N.M.: 'An automatic redesign approach for restructurable control systems', *IEEE Control Syst. Mag.*, 1985, **5**, pp. 16–22
9 PATTON, R.J.: 'Fault-tolerant control: the 1997 situation'. Proceedings of IFAC symposium SAFE-PROCESS'97, 1997, Hull, UK, pp. 1033–1055
10 BALLE, P., FISCHERA, M., FUSSEL, D., NELLS, O., and ISERMANN, R.: 'Integrated control, diagnosis and reconfiguration of a heat exchanger', *IEEE Control Syst. Mag.*, 1998, pp. 52–63
11 JIANG, J., and ZHAO, Q.: 'Design of reliable control systems possessing actuator redundancies', *J. Guid. Control Dyn.*, 2000, **23**, (4), pp. 709–718
12 ZHANG, Y.M., and JIANG, J.: 'Design of proportional-integral reconfigurable control systems via eigenstructure assignment'. Proceedings of American control conference, 2000, Chicago, USA, pp. 3732–3736
13 NOURA, H., SAUTER, D., HAMELIN, F., and THEILLIOL, D.: 'Fault-tolerant control in dynamic systems: application to a winding machine', *IEEE Control Syst. Mag.*, 2000, pp. 33–49
14 WANG, H., and WANG, Y.: 'Neural-network-based fault-tolerant control of unknown nonlinear systems', *IEE Proc., Control Theory Appl.*, 1999, **146**, (5), pp. 389–398
15 HUANG, C.Y., and STENGEL, R.F.: 'Restructurable control using proportional-integral implicit model following', *J. Guid. Control Dyn.*, 1990, **13**, (2), pp. 303–309
16 MOERDER, D.D., HALYO, N., BROUSSARD, J.R., and CAGLAYAN, A.K.: 'Application of precomputed control laws in a reconfigurable aircraft flight control system', *J. Guid. Control Dyn.*, 1989, **12**, (3), pp. 325–333
17 JIANG, J.: 'Design of reconfigurable control systems using eigenstructure assignment', *Int. J. Control*, 1994, **59**, (2), pp. 395–410
18 BODSON, M., and GROSZKIEWICZ, J.: 'Multivariable adaptive algorithms for reconfigurable flight control', *IEEE Trans. Control Syst. Technol.*, 1997, **5**, (2), pp. 217–229
19 MAYBECK, P.S., and STEVENS, R.D.: 'Reconfigurable flight control via multiple model adaptive control methods', *IEEE Trans. Aerosp. Electron. Syst.*, 1991, **27**, (3), pp. 470–479
20 GAO, Z., and ANTSAKLIS, P.J.: 'Stability of the pseudo-inverse method for reconfigurable control systems', *Int. J. Control*, 1991, **53**, (3), pp. 717–729
21 MORSE, W.D., and OSSMAN, K.A.: 'Model following reconfigurable flight control systems for the AFTI/F-16', *J. Guid. Control Dyn.*, 1990, **13**, (6), pp. 969–976
22 NAPOLITANO, M.R., and SWAIM, R.L.: 'New technique for aircraft flight control reconfiguration', *J. Guid. Control Dyn.*, 1991, **14**, (1), pp. 184–190
23 WU, N.E., ZHANG, Y.M., and ZHOU, K.: 'Detection, estimation, and accommodation of loss of control effectiveness', *Int. J. Adapt. Control Signal Process.*, 2000, **14**, (7), pp. 775–795
24 SOBEL, K.M., and SHAPIRO, E.Y.: 'A design methodology for pitch pointing flight control systems', *J. Guid. Control Dyn.*, 1985, **8**, (2), pp. 181–187
25 BROUSSARD, A.R., and O'BRIEN, M.J.: 'Feedforward control to track the output of a forced model', *IEEE Trans. Autom. Control*, 1980, **15**, (4), pp. 851–853
26 NARENDRA, K.S., and TRIPATHI, S.S.: 'Identification and optimization of aircraft dynamics', *J. Aircr.*, 1973, **10**, (1), pp. 193–199